

Design of an Autonomous Surface Vehicle (ASV) for the 2022 Maritime Robotx Challenge

Juan Pimentel, Bruno Molina, Victor Sevillano, Victor Huayapa, Sebastian Herrera, Sebastian Merino, Fernando Paz, Jaime del Alcazar, Miguel Vargas, Mario Balcazar, Manuel Escobar, Francisco Cuellar

Abstract — This paper presents the process performed by Tumiboy Team to adapt the Wave Adaptive Modular Vessel (WAM-V) to solve the RobotX challenge. This team is composed of professionals from the robotics industry in Peru and undergraduate students from the Pontifical Catholic University of Peru. The team equipped WAMV with high-precision sensors such as LiDAR sensors, RGB and Hyperspectral cameras, GPS and hydrophones, to solve the RobotX challenge. Algorithms for object recognition and path planning are in charge of obtaining sensor data, identifying objects as targets or obstacles and then deciding the movement of the vehicle. Additionally, a ball flinger mechanism was designed and implemented in order to achieve the “Find and Fling” task. After tests performed in environments such as pools and beaches, the adapted WAMV proved to be able to complete the tasks of RobotX Challenge 2022.

I. INTRODUCTION

The Maritime RobotX Challenge is a biannual international competition hosted by RoboNation that includes the participation of universities from all over the world. The challenge is to transform the Wave Adaptive Modular-Vessel (WAM-V) into an Autonomous Maritime System (AMS), developing and integrating an Unmanned Surface Vehicle (USV) and an Unmanned Aerial Vehicle (UAV). The RobotX Maritime Challenge 2022 will take place from November 11-17, at the Sydney Island International Regatta Center near Penrith in New South Wales, Australia [1].

This competition consists of a total of nine tasks in which different control, processing and communication algorithms must be implemented to solve them. Task one referred to the communication test between WAM-V and the station; Task two, three, five and six related to buoys recognition and hydrophone signal detection; Task four related to the reading of data from hyperspectral camera and; the last task eight and nine related to the use of the drone [1]. This article provides an overview of the mechatronic design used in the WAM-V. The design strategy is briefly detailed, followed by an in-depth discussion of the system design, which involves the fields of mechanical, electronic, signal processing, and control engineering.

II. DESIGN STRATEGY

The design strategy for the Tumiboy RobotX Autonomous Surface Vehicle (ASV) has 3 main pillars: modularity, reliability and simplicity.

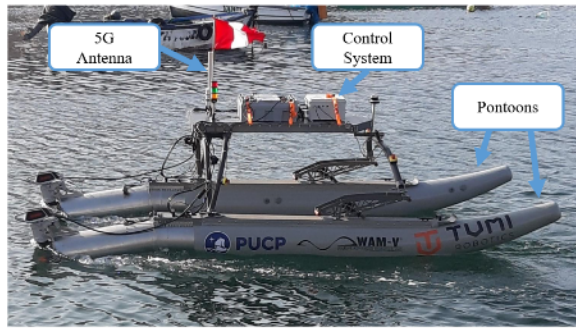


Figure 1. Tumiboy's ASV in testing grounds.

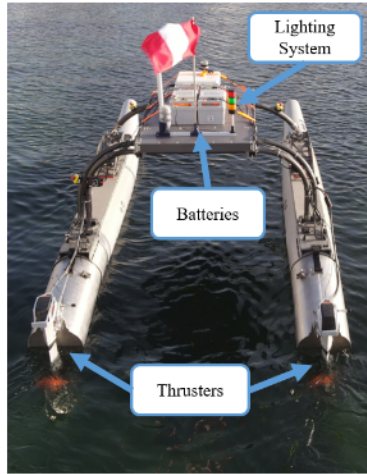
Testing grounds for the ASV were located in Pucusana, Lima, approximately 75 kilometers away from PUCP. Due to this limitation, a modular design was necessary to ensure an agile assembly and disassembly of the vehicle in every testing session. An additional benefit of this design principle was the ability to easily change the components' spatial configuration in the ASV. Transportation of the components was made easier thanks to the modular design principle which reduced the space and the time needed.

The simplicity of the ASV's design allowed for flexibility in the expansion of electric, electronic and mechanical modules during development. Racks and anchor points used to mount modules on the platform were positioned such that various spatial configurations could be used to test specific modules and capabilities of the ASV. This allowed for heavy components and modules, such as batteries and the ball launcher module, to be positioned in the center of the ASV, to minimize the effect of the additional weight in the vehicle dynamics.

Waterproof enclosures were considered to store electronics and control systems of the autonomous vehicle. These enclosures were selected to have an IP rate greater than 66. Additionally, connections between enclosures, sensors and actuators use waterproof connectors and cable glands. The software that runs algorithms for object recognition, path planning and vehicle control was mainly written in Python. Besides, ROS and Gazebo environments were used for testing purposes due to its wide use in Robotics applications and extensive documentation.



(a) Side View



(b) Back View

Figure 2. Tumiboy's ASV modules

III. SYSTEM DESIGN

The VDI 2221[2] design methodology was followed for task clarification, defining functions and designing modules. Some tasks of the WAM-V were identified as systems functions, facilitating the research about operational means. In addition, the team decided to take into consideration similar solutions which could be reused such as [3]. An overview of the Tumiboy's ASV modules is shown in Figure 3.

A. Hardware Design

This section outlines the main hardware components that will be equipped to the WAMV platform. The overview of the Control System Electronics in Diagram is shown in Figure 5.

1. Propulsion System

The AMS propulsion system consists of two power thrusters located at the rear of each pontoon. This configuration is known as a differential thrust steering, which reduces the turning radius of the vehicle allowing it essentially to turn in place. Differential thrust takes advantage of the motor's ability to apply forward and reverse thrust, in this way if the left motor is thrusting forward and the right motor on reverse then the vehicle will be turning right. Based on the experience gained in [3], two

(02) Torqeedo Cruise 2.0 were selected since they are rated for 120 lbs of thrust, allowing the vehicle to navigate at a top speed of more than 6 knots, which is enough for tasks completion. These thrusters are rated at 24V and the RS485 structured communication protocol that they have facilitates their control and a rapid detection of faults in case they occur. The propulsion system was mounted on the WAM-V platform by using a bolted joint. Due to constant salt water exposure, stainless steel bolts were used. Nylon lock nuts were included in the assembly to ensure a secure joint.

2. Electronics

For electronic design, three (03) enclosures were considered, mainly for modularity, safety and ease of assembly. Emergency stop enclosure, used for on-board or remote shutdown in case of dangerous situations. Onboard control enclosure, contains sensing, processing and communication units for autonomous operation of the vehicle. Ball flinger enclosure, handles both power and control exclusively for the use of this system.

Emergency stop system: Consists of a 14.8V 10000 mah battery, four (04) kill switches located around each WAM-V corner and an industrial wireless emergency stop button with a range of 600 meters in open field. To break-down the Torqeedo Thrusters power, a three phase contactor, rated at 24V, is used along with a step up regulator to reach a stable voltage. The electronic diagram is shown in Figure 4.

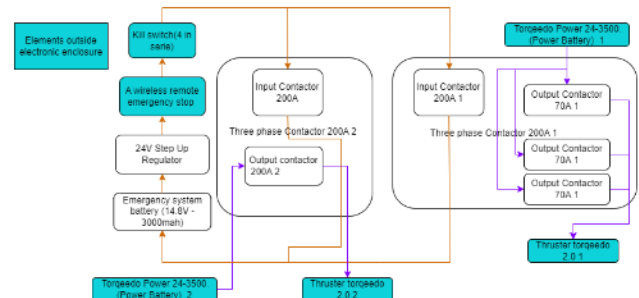


Figure 3. Emergency stop system electronic diagram.

Onboard Autonomy control system: A solid state relay is for controlling the propulsion system. Since a flight controller only outputs PWM signals, it interfaces a Nucleo STM32H745ZI microcontroller to map PWM signals into RS485 commands to control Torqeedo thrusters. The second processing unit is in charge of acquiring hyperspectral images and processing them to identify their source. Besides, they also interface with the Nucleo microcontroller to determine which beacon is emitting the sound waves and control the lighting system. Finally, it also communicates with the ground station located on shore through the Rocket router and Omnidirectional antenna to send commands that allows WAMV monitoring.

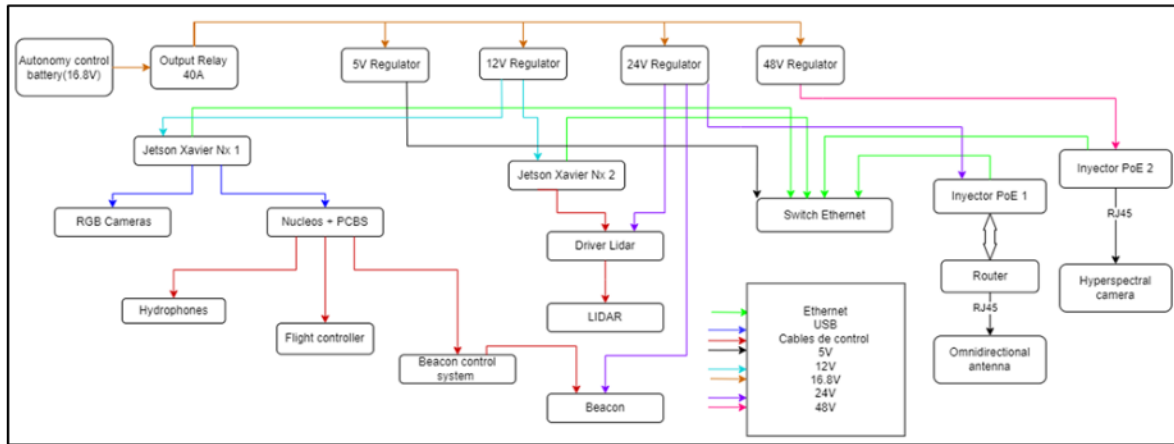


Figure 4. Onboard Autonomy Control System Electronics Diagram

Additionally, two PoE injectors are considered in order to power and transmit data through RJ45 connection to the hyperspectral camera and the Rocket M5 router.

3. Ball Finger

Task 7 of the Robotx challenge consists of flinging a racquetball towards holes located in floating platforms. To achieve this task, a mechanical system must be designed to fling a racquetball with accuracy and within a certain distance and height range. An overview of this system is shown Figure 5.

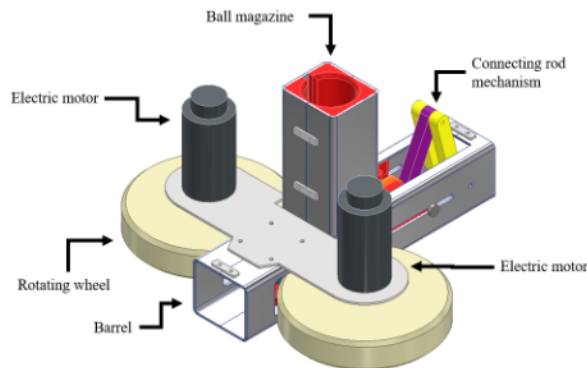


Figure 5. Ball Flinger Assembly.

The design of the ball flinger is based on two rotating wheels that will launch the ball with controlled speed and angle. The central structure of the launcher uses two bent aluminum plates which will support the weight of electric motors, the firing mechanism and the ball magazine. The firing mechanism is based on a connecting rod mechanism, such that every ball is pushed against the rotating wheels with repeatable conditions.

The “piston” of this mechanism serves two purposes: Loading balls from the magazine into the barrel, and

pushing the loaded ball into the rotating wheels. These components were designed to be fabricated using additive manufacturing. This allows a more organic design which is more suited for a surface that will be in contact with the ball. Additionally, fine tuning via testing of these contact surfaces was a less time-consuming process, due to the high speed process of additive manufacturing.

In order to select the electric motors which actuate the rotating wheels, a rotating speed was calculated such that the inertia of the rotating wheels would launch the racquetballs, and not the available torque of the electric motors. To perform a successful ball fling, two parameters must be set for the ball launcher: Angle on Z-axis and wheel speed. The combination of these parameters allows firing racquetballs towards any target in an 8 meters range.

The electronic system of the Ball Flinger, which is shown in Figure 6, consists of a battery, four actuators: two DC Dunkermotoren GR63x65 motors to activate the rotating wheel, one servomotor RMD-X8 actuator for steering the Ball Flinger and another servomotor A6380 for charging the racquetballs. Besides, a microcontroller is considered to receive commands from the control system and execute the launching task.

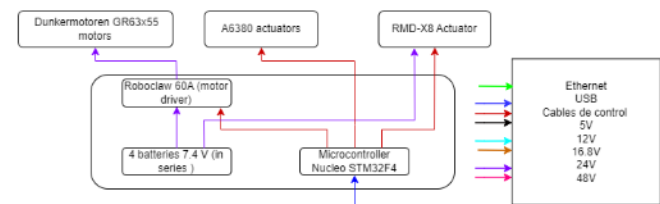


Figure 6. Ball Flinger system electronic diagram

4. Buoys Detection

The selected components correspond to a 32-channel Ouster lidar (OS1-32), which has a vertical field of view of 45°; and LifeCam HD-3000 cameras. Below is the positioning of the lidar and the two cameras. As shown in figure 7, the lidar is attached at the top by bolts to a 3D printed base. Regarding the cameras, these are positioned, below the lidar, in two 3D pieces which are fixed to the v-slot bar by bolts. The separation between the cameras maintains a fixed angle of 30°.

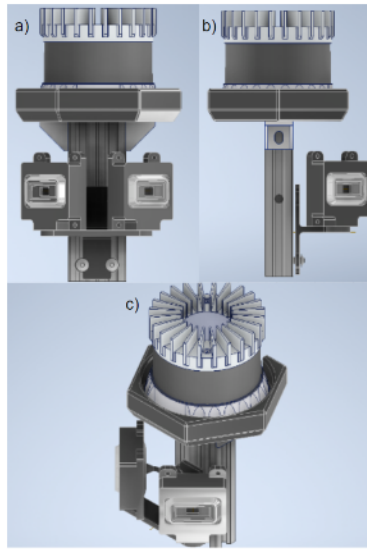


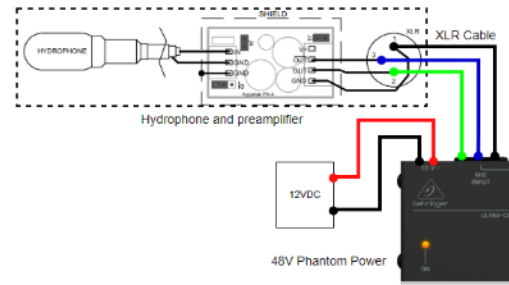
Figure 7. a) Side view of support. b) Front view of support. c) Lidar and camera support

5. Local Network

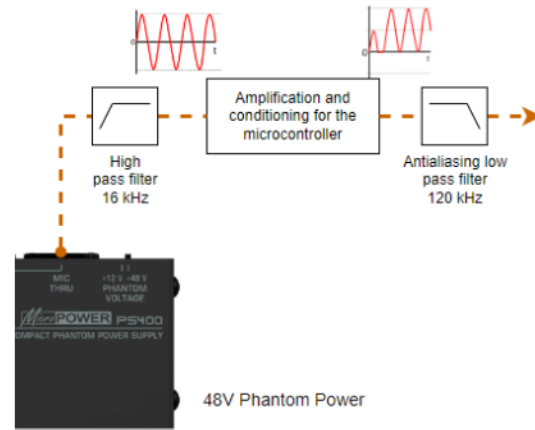
In order to ensure stable and long-range wireless communication between the WAMV and the Operator Control Station (OCS), the use of an Ubiquitous Rocket M5 Router together with an AMO5G13 omnidirectional antenna was considered. Additionally, a switch was installed to create a local network allowing interconnection and of multiple ethernet devices, such as Jetson Xavier Processors, Lidar and Hyperspectral Camera.

6. Beacon and Hydrophones

The identification of underwater beacons is a critical task for correctly tracing the path of the WAM-V through the gates. As mentioned in the Team Handbook [1], the frequency range of the beacon's signal varies between 25 kHz to 40 kHz and is transmitted every 0.5 Hz to 2 Hz. The connection diagram for one hydrophone is presented in Figure 8. Since the WAM-V carries two hydrophones, two independent circuits with similar design are used.



(a) Phantom Power input



(b) Phantom Power output

Figure 8. Connection diagram

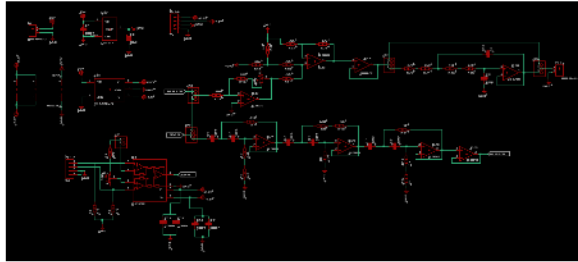
Each hydrophone is connected to a preamplifier with a fixed gain that can be set to 6 dB or 20 dB. Then, the preamplifier is connected to a Phantom Power that improves the Signal to Noise Ratio (SNR) and increases the hydrophone sensitivity. Finally, the Phantom Power output is processed with analog circuitry including a 20 kHz 6th order high pass filter for low frequency noise, a conditioning circuit for the microcontroller, and a 100 kHz 2nd order antialiasing low pass filter.

To emulate the beacon's behavior, an ultrasonic waterproof sensor was tested. This kind of sensor is found in almost every light vehicle to avoid collisions while parking and it can transmit a 40 kHz signal at 20 ms rate. The sensor chosen for the tests is shown in Figure 9.

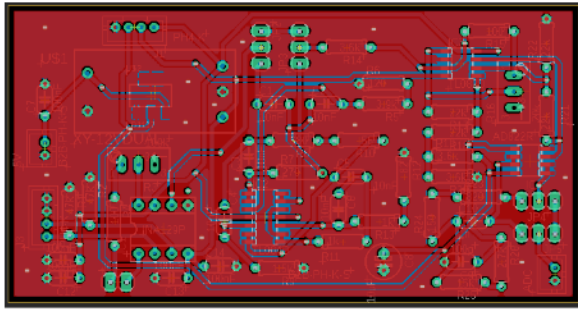


Figure 9. Waterproof ultrasonic sensor

The schematic and board layout, which are shown in Figure 10, were designed based on the connection diagram presented before. An INA129 is used for the differential Phantom Power output. This device removes the common noise between its two inputs. In this case, one is the signal and the other one is an inverted version of it. Then, the INA's output is connected to the high pass filter composed by a TL084 JFET input Op-Amps. Later, a TL082 is used to amplify and add a 1.6 VDC offset for the microcontroller ADC input. Finally, the antialiasing filter is placed between the conditioning circuit and the ADC.



(a) Schematic



(b) Board Layout

Figure 10. Filters and conditioning circuitry

B. Software Design

This section outlines the main software design that will be considered for processing techniques and vehicle control algorithms.

7. Communication Protocol

The communication protocol is achieved by socket communication, where the server is located in the WAMV and the client is the OCS, this is due to the ease with which the client can write messages and the server only answers. The operation is as follows, from the client a message is sent to the server, which receives what task it is in and the WAM-V sends the required messages. It is also part of the task to replicate this message to the Technical Director Server via Ethernet. To achieve this from the OCS, the request-post method was used, which requires an IP address and a port to send these messages to periodically.

Finally, an additional requirement was to display the data on a local web page, which shows the last 10 messages that have been received and is updated without the need to reload the page. The messages received in the webpage are shown in Figure 11.

RobotX PUCP Home

#	Mensaje
1	\$RXHRB,290922,002357,21.31198,N,157.88972,W,ROBOT,2,1*1F
2	\$RXHRB,290922,002358,21.31198,N,157.88972,W,ROBOT,2,1*10
3	\$RXHRB,290922,002359,21.31198,N,157.88972,W,ROBOT,2,1*11
4	\$RXHRB,290922,002400,21.31198,N,157.88972,W,ROBOT,2,1*1A
5	\$RXHRB,290922,002401,21.31198,N,157.88972,W,ROBOT,2,1*1B
6	\$RXHRB,290922,002402,21.31198,N,157.88972,W,ROBOT,2,1*18
7	\$RXHRB,290922,002403,21.31198,N,157.88972,W,ROBOT,2,1*19
8	\$RXHRB,290922,002404,21.31198,N,157.88972,W,ROBOT,2,1*1E
9	\$RXHRB,290922,002405,21.31198,N,157.88972,W,ROBOT,2,1*1F
10	\$RXHRB,290922,002406,21.31198,N,157.88972,W,ROBOT,2,1*1C

Figure 11. Web page results

8. Buoys Detection

Regarding the processing of the images captured by the camera, the algorithm to recognize buoys follows stages shown in Figure 12. An example is presented in Figure 13.

The automatic recognition of buoys begins with the equalization of the image, which makes it uniform from its probability distribution function; thus, improving its visualization in conditions where the image is blurred. Then, it proceeds to use the blue plane which will be used to differentiate the color of the sea from the rest of the objects. Once the plane is selected, it is filtered with a low pass that will reduce the sharp edges of smaller size (such as the edges of sea currents). Canny algorithm is applied for edge detection [4]. The area is then thresholded to remove small segments. Finally, the centroid of the detected elements is positioned. The results of two images are shown below. The first contains a set of red buoys linked in a row [5].

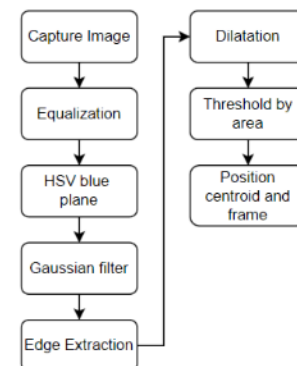


Figure 12. Scheme for the detection of buoys with the camera

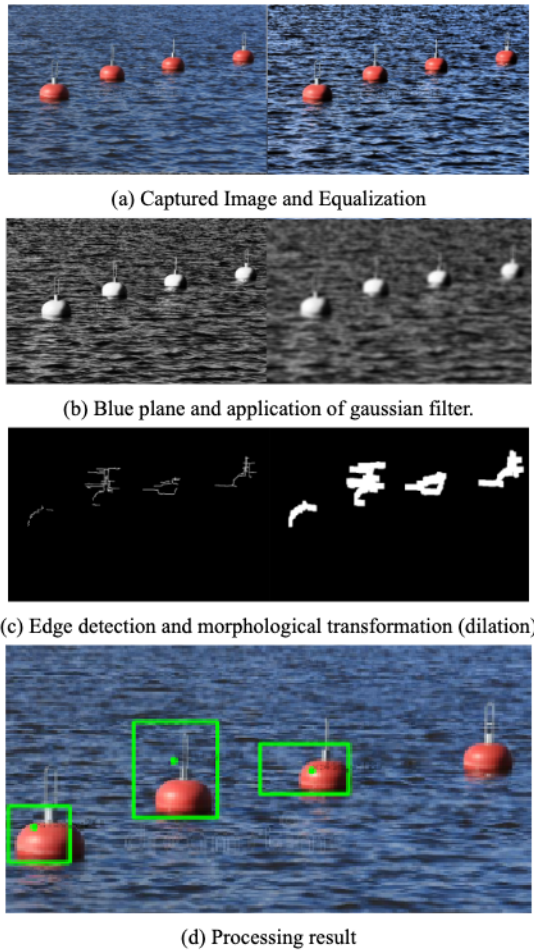


Figure 13. Results of processing algorithm for red buoys detection

Lidar: The structured representation of the point cloud allows the generation of matrices of distance and reflectivity, which can be treated as images. Correctly delimiting the numerical values of the matrix allows the rescaling of image intensities, in grayscale, to be more pronounced. With this, the pressure of objects increases. The proposed scheme to treat the lidar data is shown in Figure 14, and the comparison between raw data and filtered data is shown in Figure 15.

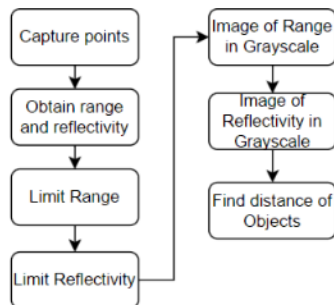


Figure 14. Scheme proposed to data's lidar

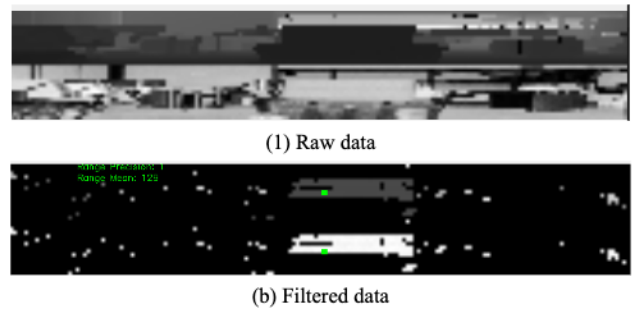


Figure 15. Comparison between raw and filtered data

The recognition of the buoys shape and color are part of the process to correctly complete tasks 2 and 3 of the challenge. For this purpose, a Lidar and an RGB camera are used to calculate WAM-V's next point of positioning. Said value is known due to the Match between the result of the processing applied to the camera image and the grayscale image of the lidar. Figure 16 shows the proposed scheme to locate these points. The Match between both devices was obtained proportionately limiting the 360° data capture of the lidar to 60° of each of the cameras.

Once the camera recognizes that this object corresponds to a buoy and the lidar finds the distance of objects, then the next step is to calculate the point X_f and Y_f (as shown in Figure 17). After this process, intermediate points are calculated to ensure a smooth movement of the WNV. When the robot reaches the end point, the schema is processed again.

9. Vehicle control

The Orange Cube autopilot flight controller was used to perform vehicle movement control. Information from its Inertial Measurement Units and a Here3 GPS is integrated to estimate position in a local North-East-Down frame of reference. The autopilot was previously configured so the vehicle is considered as a boat, which is a class of the Rover frame. This allows the vehicle to maintain a fixed position or to move to a desired position by setting two PWM outputs to control the thrusters.

The vehicle is commanded using guided mode, which consists of constantly receiving messages from the Ground Station which contain position and orientation targets. In this case, the Jetson behaves as the Ground Station for the autopilot and commands are sent through a USB cable following the Mavlink communication protocol. Targets are obtained from the buoy detection algorithm in a local frame of reference and frame conversion is performed to generate the message using the orientation estimated by the autopilot.

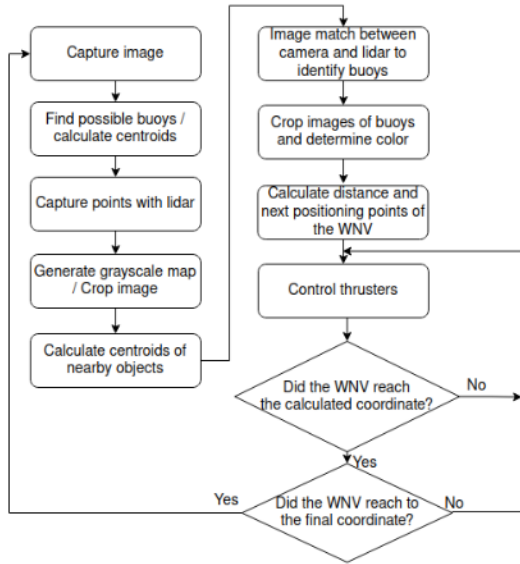


Figure 16. Scheme to determine a next point

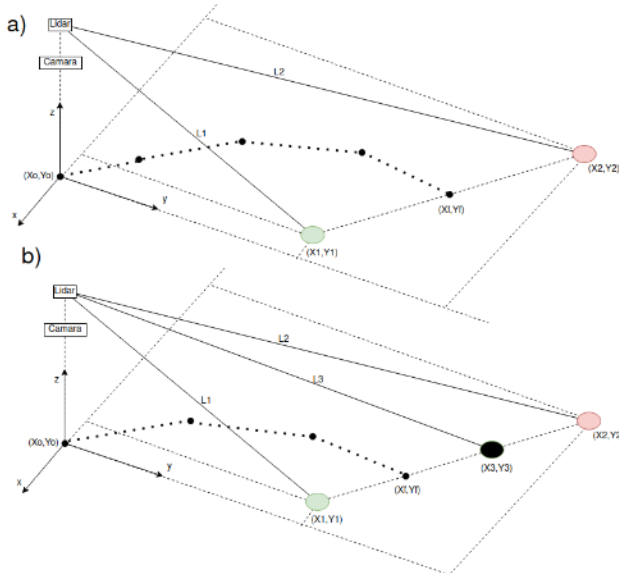


Figure 17. Intermediate points between WAM-V's position and the final point with two and three buoys.

10. Hyperspectral Camera

The HSI camera provided by RobotX is used to distinguish the different wavelengths present in its field of view. Since this is a line scan camera, it is important to consider the exposure time and the speed at which the boat is moving. Figure 18 shows the image obtained from the camera.

For comparison with paintings depicting animals during the competition, reflectance will be used instead of radiance, thus avoiding dealing with how radiance changes with light. The equation (1) shows how to obtain α , that is the angle formed between the reference spectrum and the image spectrum, and the smallest angle represents the greatest similarity between the curves.

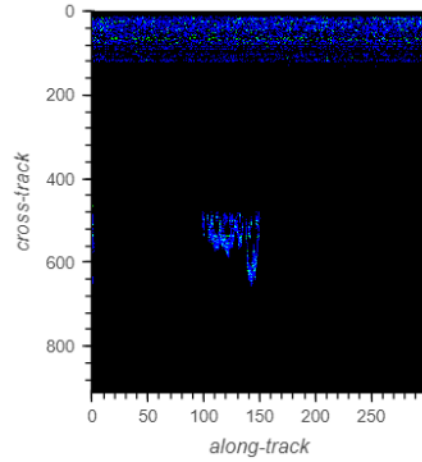


Figure 18. Image obtained by the HSI camera

$$(1) \quad \alpha = \cos^{-1} \left(\frac{\sum \text{Image Spectrum} * \text{Reference Spectrum}}{\sqrt{(\sum \text{Image Spectrum})^2 * (\sum \text{Reference Spectrum})^2}} \right)$$

11. Audio signal processing

In order to condition the hydrophones signals to the frequency range of interest two filter blocks were considered. The first is a 6th order 16 kHz high pass filter that will remove the noise generated from the motors or other low frequency sounds coming from the environment. The second one is a 2nd order 120 kHz low pass antialiasing filter that removes any unwanted harmonics due to sampling frequency of the microcontroller's ADC.

A 100 kHz sampling frequency is used for the beacon's 45 kHz maximum frequency. The microcontroller includes 3xADCs with 16-bit maximum resolution up to 3.6 MSPS. These characteristics are important because they will determine how well the signal is digitally reconstructed.

IV. EXPERIMENTAL RESULTS

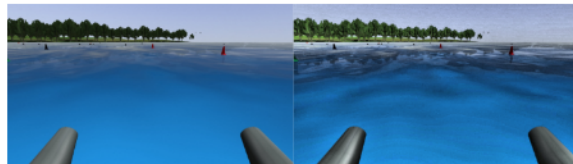
This section describes results obtained during tests and performed in both water and simulated environments (ROS and Gazebo) of vehicle's navigation, remotely operated and autonomous, image and point cloud processing algorithms and acoustic waves detection.

During on-water testing, the vehicle's remote operation was firstly tested, aspects such as maneuverability and ease of use were taken into account for this evaluation. Pucusana beach was considered as a test environment due to the high presence of boats and waves. This allowed us to demonstrate the correct remote operation of the vehicle under extreme conditions. Besides, this test verified the mechanical resistance of the support elements for the Lidar, cameras, antenna, beacon. Figure 19 shows the ASV at the point of being deployed on the Pucusana beach

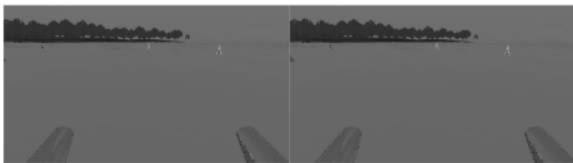


Figure 19. ASV in Pucusana beach, Lima - Peru.

The buoys detection algorithm was tested in the Gazebo simulation environment [6]. Through the image_view topic, the three cameras of the simulated WAM-V were accessed, in which the algorithm was executed. The results are presented in the following figure.



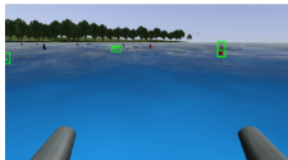
(a) Captured Image and Equalization



(b) Blue plane and application of gaussian filter.



(c) Edge detection and morphological transformation (dilation)



(d) Processing result

Figure 20. Results of processing algorithm for buoys detection in Gazebo. Additionally, as a result of the filtering and amplification process made for the hydrophones, the signal could be seen through the oscilloscope. Fine tuning is required to achieve the desired output signal. Figure 21 and Figure 22 show the parameters that were measured at the high pass filter output: frequency and pulse rate.

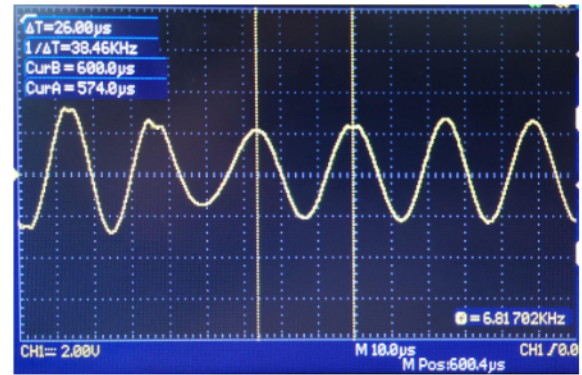


Figure 21. Signal frequency

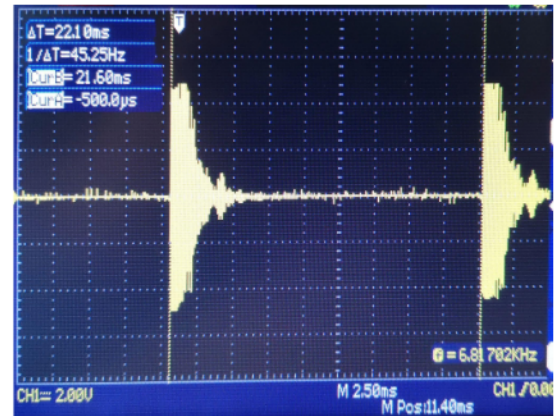


Figure 22. Signal pulse rate

V. CONCLUSIONS

This document presents the process, done by the team Tumiboy, to adapt the Wave Adaptive Modular Vessel (WAM-V) into an Autonomous Superficial Vehicle (ASV) to achieve the tasks of the RobotX challenge. For the development of this work, the team took as a reference the works presented in previous challenges along with similar projects developed locally. From a mechanical perspective the focus was on solutions principles and design; for example, for the Ball Flinger task, the solution principle used two rotating wheels while the design considered the motors, structure, material, size, among others. For autonomous navigation, programming and control algorithms were needed to solve the tasks. In addition, for the electric/electronic operational means the development focused on signal acquisition and image processing as well as the modularity and physical layout of these devices. Emergency system, object recognition, path planning, ball flinger module, hyperspectral camera were sections that demanded additional work. Currently, an intermediate degree of autonomy has been achieved. Future work will improve the level of autonomy of this vehicle and develop better filtering and processing techniques.

VI. ACKNOWLEDGEMENTS

Team Tumiboy would like to acknowledge the Pontifical Catholic University of Peru for the financial support and documentation management, and Tumi Robotics for providing the work space as well as facilitating the equipment transport, in addition to travel expenses.

VII. REFERENCES

- [1] Robotx CHALLENGE, "2022 TEAM HANDBOOK", 2022
- [2] VDI-Fachbereich Produktentwicklung und Mechatronik. "VDI Standard: VDI 2221 Systematic approach to the development and design of technical systems and products." Germany, 1993.
- [3] L. Velasco, J. Balbuena, J. Gonzales and F. Cuellar, "Development of an ASV for Oceanographic Monitoring on the Huarmey Coast," *2021 IEEE 30th International Symposium on Industrial Electronics (ISIE)*, 2021, pp. 1-7, doi: 10.1109/ISIE45552.2021.9576371.
- [4] Lynn, N. D., Sourav, A. I., & Santoso, A. J." Implementation of Real-Time Edge Detection Using Canny and Sobel Algorithms". 2021 In IOP Conference Series: Materials Science and Engineering (Vol. 1096, No. 1, p. 012079). IOP Publishing.
- [5] Dreamstime. Red buoys on the water [Online]. Available: <https://www.dreamstime.com/four-red-buoys-water-red-buoys-water-image-105261432>
- [6] Open Robotics (2021, Set 10). vrx_2022 perception_task [Online]. Available: https://github.com/osrf/vrx/wiki/vrx_2022-perception_task
- [7] A. Osmar and M. Paulo. "Spectral Correlation Mapper (SCM): An Improvement on the Spectral Angle Mapper (MAP)" , Departamento de Geografia da Universidade da Brasilia..